International Journal of Solids and Structures 49 (2012) 2559–2567

Contents lists available at SciVerse ScienceDirect

International Journal of Solids and Structures

journal homepage: www.elsevier.com/locate/ijsolstr

Stability and optimal shape of Pflüger micro/nano beam

V.B. Glavardanov *, D.T. Spasic, T.M. Atanackovic

Department of Mechanics, University of Novi Sad, P.O.B 55, 21121 Novi Sad, Serbia

ARTICLE INFO

Article history:
Received 16 January 2012
Received in revised form 17 February 2012
Available online 30 May 2012

Keywords:
Non-local beam
Nanostructures
Stability
Pontryagin's principle
Optimization

ABSTRACT

This paper deals with optimal shapes against buckling of an elastic nonlocal small-scale Pflüger beams with Eringen's model for constitutive bending curvature relationship. By use of the Pontryagin's maximum principle the optimality condition in form of a depressed quartic equation is obtained. The shape of the lightest (having the smallest volume) simply supported beam that will support given uniformly distributed follower type of load and axial compressive force of constant intensity without buckling, is determined numerically. A special attention is paid to the influence of the characteristic small length scale parameter of the nonlocal constitutive law to both critical load and optimal shape of the analyzed beams. For the case when distributed follower type of load is zero, our results reduce to those obtained recently for compressed nonlocal beam. Also the post buckling shape of the optimally shaped rod is studied numerically.

1. Introduction

Lately there is considerable effort devoted to the study of stability of nano beams. Nano beams are modeled within the framework of second grade elasticity and within integral-based nonlocal theories. While the classical elasticity is size independent, generalized theories, allow one to account for the length scale that becomes important in micro/nano structures.

According to Ma et al. (2008) one of the first papers, based on the integral, non-local constitutive relation, suggested by Eringen (1983), could be related to work of Peddieson et al. (2003) who developed a non-local model for Bernoulli–Euler beams. This model is a suitable alternative to size-independent classical continuum elasticity for applications at the nanoscale, where the discrete atomistic nature of matter becomes important. Recently there has been a number of studies of buckling of nonlocal nano beams. We list some of them. Buckling analysis of multi walled carbon nano tubes is treated in Sudak (2003). Wang et al. (2006) formulated a nonlocal Timoshenko beam theory (a theory that takes into account transverse shear deformation) and applied it to a buckling analysis of a beam with constant cross-section and different boundary conditions. In Lu et al. (2007) the equations of motion for nonlocal Euler and Timoshenko beams are derived. Those equations are then applied to the study of wave propagation of a single and double walled nano tubes. The results presented in Lu et al. (2007) are suitable for the dynamic stability study of nano tubes. In Wang and Wang (2007) the constitutive equations for the carbon nano tubes as Euler–Bernoulli and Timoshenko beams are presented. Again analysis was based on Eringer's nonlocal theory. Finally we mention the work of Challamel and Wang (2010) where the lateral buckling of nano beams with constant cross-section was studied.

The stability analysis of a nano beam subjected to a nonconservative load (generalized Beck's problem) has been presented in Xiang et al. (2010), while the flow induced vibrations are treated in Ke and Wang (2011). As stated in Lu et al. (2007), it is necessary to address basic issues governing the nonlocal theories. The question of optimally shaped rod is, in our opinion, an important issue and we address it here.

The problem of determining optimal shape against buckling of a nano rod, was treated, for the first time, in Atanackovic et al. (in press) and Atanackovic et al. (2012). It was shown in these works that the Pontryagin's principle may be used successfully to determine the shape of the rod that has minimal volume (mass) and is stable under the action of a prescribed force. There is considerable increase in the buckling load for optimally shaped rod made of given amount of material when compared with the rod with constant cross-section. Our intention in this work is to study stability and optimal shape of a nano beam loaded by an axial compressive force and distributed type follower load. Thus, we consider a generalization of a classical Pflüger beam.

We give a motivation for studying this problem. Due to the recent development of technology (MEMS and NEMS) the analysis of micro/nano beams have become a very interesting field of research. The investigation of mechanical behavior of such beams is performed by the use of molecular dynamics simulations or continuum mechanics models. The molecular dynamic simulations are very difficult for large scale systems. Since we are interested in

* Corresponding author. Address: Trg Dositeja Obradovica 6, P.O.B 55, 21121 Novi Sad, Serbia. Tel.: +381 21 485 2251; fax: +381 21 458 133.
E-mail address: vanja@uns.ac.rs (V.B. Glavardanov).

0020-7683/$ - see front matter © 2012 Elsevier Ltd. All rights reserved.
http://dx.doi.org/10.1016/j.ijsolstr.2012.05.016

formulating the general procedure applicable to both large scale (the length scale parameter tending to zero) and small scale systems the use of the continuum mechanics models is chosen. In particular this means that we will use the nonlocal elasticity theory suggested by Eringen (1983). We give next the physical examples corresponding to the mathematical model that will be used. As the first example of the beam with uniformly distributed follower loads we mention pipes conveying fluid (Plaut, 2004). We note that the physical behavior of the fluid in macro/micro systems is different from the behavior inside nano pipes. However, in order to obtain at least qualitative results some authors neglected the above mentioned differences and treated a nano pipe in the same way as a macro/micro pipe (Lee and Chang, 2008; Wang, 2009; Tounsi et al., 2009). In what follows we will use this approach. As the second example we mention a nano beam in the air or fluid flow. This situation occurs in many nano/micro electronic devices (air is used as a cooling medium). We note that the stability boundary of a uniform Pflüger nano beam, pined at both ends, could be used to determine the stability boundary of the shearable (Timoshenko) uniform Pflüger macro beam since the governing equations have the same structure. This conclusion is reached in Wang et al. (2006). Besides investigating stability, the aim of the paper is to give an insight into the influence of the size of the beam on the optimal shape and savings in material. Since the optimal shape of a compressed Pflüger macro beam has not been analyzed yet, the analysis presented here, having small length scale parameter, will cover macro, micro and nano beams. This will, potentially, help engineers chose whether it pays off to use, or not to use, the optimal shaped beam. Besides that, an interesting physical phenomena, connected to regularization of the optimal solution, will also be presented in the present work. Giving the motivation for the problem treated here we continue by briefly describing the main ideas of the paper.

Optimal shape of such a beam within the classical Bernoulli–Euler theory was presented in Atanackovic and Simic (1999). In solving our problem we will be faced with two problems. First we will determine the critical load parameters (axial force and intensity of distributed follower force) for a nano beam with constant cross-section. We believe that this is a new result. Those load parameters are obtained in closed form. When dealing with critical buckling loads, according to Kovari (1969) the advantages of closed form solutions are lessened by the need to solve complicated transcendental equations generated by boundary conditions. That these equations must be solved numerically suggests that a far more efficient process would be to give the original boundary value problem a numerical treatment *ab initio*. Thus besides the standard procedure that involves theory of holomorphic functions we will apply the numerical method presented in Goodman (1965). For engineering applications this quite efficient successive iterations method seems to be more efficient and will be used in determining the critical load parameters given in form of interaction curves for several values of the small length scale parameter of nonlocal constitutive law.

Next we will use the Pontryagin's maximum principle to determine the optimality conditions. We will show that the optimality condition determining the optimal shape of the micro/nano beam takes the form of a depressed quartic equation. Note that generalizations of the classical elastica theory, like the one at hand, lead to more complicated two point boundary value problems since optimality conditions are given in the form of polynomials. For example, see Spasic and Glavardanov (2009) where the posed boundary value problem requires a solution of the cubic equation and where its explicit solution, that determines optimal shape, was shown in terms of the Chebishev radicals. Thus, in obtaining a numerical solution that determines the optimal shape of a micro/nano beam for given arc length, in each iteration one solve the depressed quartic equation explicitly by the use of Ferrari's method. Since this procedure requires to many "if then else" conditions in each step of integration we will proceed differently. Namely, we will treat the optimality condition as a first integral and use it to solve one state variable. Also we will differentiate it to obtain the relation that connects changes of optimal cross section with respect to the remaining state variables. When compared to numerical procedure that involves the Ferrari solution, the suggested procedure is more efficient.

Finally we will determine the post-critical shape of an optimally shaped beam by numerical integration of the corresponding equilibrium equations.

2. Mathematical formulation of the problem

Consider a simply supported, naturally straight beam BC of length L. In order to derive governing equations we define the rectangular Cartesian coordinate system xBy whose axis x coincides with the beam axis in the undeformed state while the y axis is perpendicular to the x axis (see Fig. 1). Also we introduce the arc length of the beam axis in the undeformed state S measured from the fixed end B. In deriving the governing equations we assume that the beam has a variable cross sectional area $A = A(S)$. At the movable end C, the beam is loaded by a concentrated force $\boldsymbol{F}$ of constant intensity F acting along the x axis. Also the beam is loaded by a uniformly distributed follower type of load of constant intensity say q_0.

The corresponding differential equations describing the equilibrium of the beam element of length dS (see detail in Fig. 1) read

$$\frac{dH}{dS} = -q_x, \quad \frac{dV}{dS} = -q_y, \quad \frac{dM}{dS} = -V\cos\theta + H\sin\theta, \tag{1}$$

where H, V are the components of the contact force along the x and y axes, respectively, M is the contact couple, θ is the angle between the tangent to the beam axis and the x axis and q_x and q_y are the projections of the uniformly distributed follower type of load q_0 to the coordinate axes. Since

$$q_x = -q_0\cos\theta, \quad q_y = -q_0\sin\theta,$$

Eq. (1) becomes

$$\frac{dH}{dS} = q_0\cos\theta, \quad \frac{dV}{dS} = q_0\sin\theta, \quad \frac{dM}{dS} = -V\cos\theta + H\sin\theta. \tag{2}$$

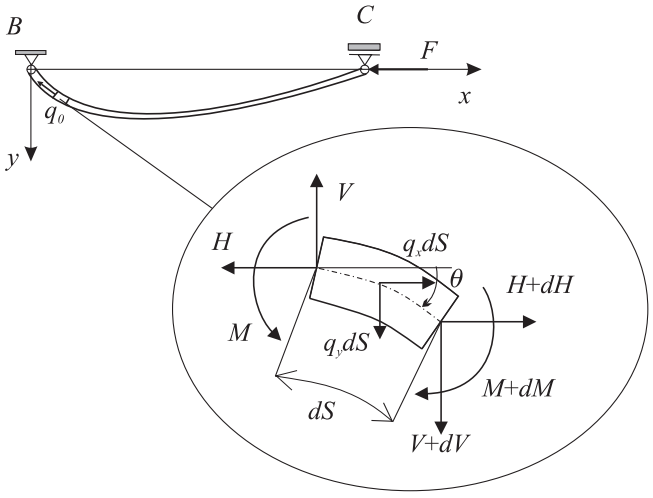

Fig. 1. System under consideration.

To the system (2) we adjoin the following geometrical relations

$$\frac{dx}{dS}=\cos\theta,\quad \frac{dy}{dS}=\sin\theta. \tag{3}$$

Following the lines of the nonlocal Eringen elastica theory the constitutive equation suitable for micro/nano beam-like structures reads (Peddieson et al., 2003; Sudak, 2003; Wang et al., 2006; Challamel and Wang, 2010).

$$M(S)-l_c^2\frac{d^2M}{dS^2}=EI\frac{d\theta}{dS}, \tag{4}$$

where l_c is the small length scale parameter of nonlocal constitutive law that is appropriate to the material and that can be identified from atomistic simulations or by using dispersive curve of the Born–Karman model of lattice dynamics as mentioned in the above listed references. In (4) EI stands for the bending rigidity of the beam i.e. Young's modulus E multiplied by the second moment of area I. It is worth noting that the system consisting of (2)–(4) can be transformed into a more convenient form for further analysis. Namely, by differentiating $(2)_3$ and using $(2)_{1,2}$ and (4) we get the following system of six first order ordinary differential equations

$$\begin{aligned}&\frac{dH}{dS}=q_0\cos\theta,\quad \frac{dV}{dS}=q_0\sin\theta,\quad \frac{dM}{dS}=-V\cos\theta+H\sin\theta,\\&\frac{dx}{dS}=\cos\theta,\quad \frac{dy}{dS}=\sin\theta\quad \frac{d\theta}{dS}=\frac{M}{EI+l_c^2(H\cos\theta+V\sin\theta)}.\end{aligned} \tag{5}$$

The boundary conditions corresponding to Eq. (5) are

$$\begin{aligned}&x(0)=0,\quad y(0)=0,\quad y(L)=0,\quad H(L)=-F,\\&M(0)=0,\quad M(L)=0.\end{aligned} \tag{6}$$

Since the beam has a variable cross-sectional area its volume W reads

$$W=\int_0^L A(S)dS. \tag{7}$$

In what follows we take the following form of the second moment of area

$$I(S)=\gamma A^2(S). \tag{8}$$

We note that the constant denoted by γ depends on the shape of the cross section. For example, in the case of circular cross section $\gamma=1/(4\pi)$. In the following we use $A_u=A(S)=const.$, for $S\in[0,L]$, to denote the cross-sectional area of the uniform beam to which the optimal one, with the same stability boundary, will be compared. In this case the second moment of area is $I_u=\gamma A_u^2$.

We can now introduce the following dimensionless quantities

$$\begin{aligned}&t=\frac{S}{L},\quad \xi=\frac{x}{L},\quad \eta=\frac{y}{L},\quad \overline{A}=\frac{A}{L^2},\quad \overline{A}_u=\frac{A_u}{L^2}\\&a=\frac{\overline{A}}{\overline{A}_u},\quad \kappa=\frac{l_c}{L},h=\frac{HL^2}{EI_u},\quad \nu=\frac{VL^2}{EI_u},\quad m=\frac{ML}{EI_u},\\&\lambda_1=\frac{FL^2}{EI_u},\quad \lambda_2=\frac{q_0L^3}{EI_u},\quad w=\frac{W}{A_uL}.\end{aligned} \tag{9}$$

By using (9) the system (5) becomes

$$\begin{aligned}&\dot h=\lambda_2\cos\theta,\quad \dot\nu=\lambda_2\sin\theta,\quad \dot m=-\nu\cos\theta+h\sin\theta,\\&\dot\xi=\cos\theta,\quad \dot\eta=\sin\theta,\quad \dot\theta=\frac{m}{a^2+\kappa^2(h\cos\theta+\nu\sin\theta)},\end{aligned} \tag{10}$$

where a dot over the variable represents the derivative with respect to the dimensionless arc length t. The boundary conditions (6) now read

$$\begin{aligned}&\xi(0)=0,\quad \eta(0)=0,\quad m(0)=0,\quad \eta(1)=0,\\&h(1)=-\lambda_1,\quad m(1)=0.\end{aligned} \tag{11}$$

In obtaining (10) we used $EI/EI_u=E\gamma A^2(S)/\left(E\gamma A_u^2\right)=a^2$. Eqs. (10) and (11) describe the nonlinear equilibrium equations of the Pflüger beam based on Eringen's nonlocal elasticity theory. Note that the classical Bernoulli–Euler elastica theory is obtained as a special case for $\kappa=0$ (Atanackovic, 1997).

The dimensionless volume is given by

$$w=\int_0^1 a(t)dt. \tag{12}$$

Since we are interested in stability and the optimal shape against buckling, it is necessary to define a solution to Eqs. (10) and (11) whose stability will be investigated. It can be seen that for fixed κ and any (λ_1,λ_2) the system (10) and (11) has the solution $h_0=-\lambda_1-\lambda_2(1-t)$, $\nu_0=0$, $\xi_0=t$, $\eta_0=0$, $m_0=0$, $\theta_0=0$, in which the beam axis remains straight. By introducing small perturbations $\Delta h,\dots,\Delta\theta$, solutions to (10) and (11) can be expressed as $h=h_0+\Delta h,\dots,\theta=\theta_0+\Delta\theta$. Substituting these into the system (10), (11) and omitting Δ in front of $\Delta\nu,\Delta m,\Delta\eta,\Delta\theta$ we obtain

$$\begin{aligned}&(\Delta\dot h)=\lambda_2(\cos\theta-1),\quad \dot\nu=\lambda_2\sin\theta,\\&\dot m=-\nu\cos\theta+[\Delta h-\lambda_1-\lambda_2(1-t)]\sin\theta,\ (\Delta\dot\xi)=\cos\theta-1,\\&\dot\eta=\sin\theta,\ \dot\theta=\frac{m}{a^2+\kappa^2\{[\Delta h-\lambda_1-\lambda_2(1-t)]\cos\theta+\nu\sin\theta\}}\end{aligned} \tag{13}$$

subject to

$$\begin{aligned}&\Delta\xi(0)=0,\quad \eta(0)=0,\quad m(0)=0,\quad \eta(1)=0,\\&\Delta h(1)=0,\quad m(1)=0.\end{aligned} \tag{14}$$

Note that the system (13) and (14) possesses the trivial solution $\Delta h=\nu=\Delta\xi=\eta=m=\theta=0$. The linearized system that will be used for determining the buckling load and optimal shape follows by neglecting the higher-order terms in (13). In this way we get

$$\begin{aligned}&(\Delta\dot h)=0,\quad \dot\nu=\lambda_2\theta,\quad \dot m=-\nu-[\lambda_1+\lambda_2(1-t)]\theta,\\&(\Delta\dot\xi)=0,\quad \dot\eta=\theta,\quad \dot\theta=\frac{m}{a^2-\kappa^2[\lambda_1+\lambda_2(1-t)]}\end{aligned} \tag{15}$$

subject to (14).

3. Critical buckling load

In order to determine the stability boundary of the beam for fixed κ, we intend to determine the values of the load parameters (λ_1,λ_2) for which the system (13) and (14) has more than one solution in every neighborhood of (λ_1,λ_2). Note that bifurcation points of the nonlinear system (13) and (14) are bifurcation points of the linearized system (15) and (14). To be sure that the bifurcation points of the linearized system are also bifurcation points of the nonlinear system some sufficient conditions should be formulated. In what follows we assume that these conditions are satisfied and note that checking of them could be done along the lines of Chow and Hale (1982), for example by following the standard procedure of Liapunov–Schmidt reduction. We will not be concerned with this analysis here. From now on we assume that $a(t)$ is a positive and continuously differentiable function.

Therefore in order to find the buckling loads we need to determine the eigenvalues of the system (15) and (14). Note that this can be done only by using $(15)_{2,3,6}$. Namely, by differentiating $(15)_3$ and using $(15)_{2,6}$ we obtain that the critical load of the Pflüger beam is determined if the following equation

$$\ddot m+\frac{\lambda_1+\lambda_2(1-t)}{a^2-\kappa^2[\lambda_1+\lambda_2(1-t)]}m=0 \tag{16}$$

subject to

$$m(0)=0,\quad m(1)=0 \tag{17}$$

has a nontrivial solution. In order to derive (16) we assumed that the following holds

$$a(t) > \kappa\sqrt{\lambda_1 + \lambda_2(1-t)}, \tag{18}$$

which makes sense since κ is the small length scale parameter. For the linear eigenvalue problem, the eigenfunctions are determined up to a multiplicative constant. Hence, it is permissible to chose

$$\dot{m}(0) = 1, \tag{19}$$

which fixes this constant. Then since the function multiplying m in (16) is analytic in $[0,1]$by applying the arguments of Whittaker and Watson (1966), we conclude that the linear differential equation (16) with the initial conditions $(17)_1$ and (19) has a unique solution. In the special case when $\kappa = 0$, corresponding to the classical elastica theory, the problem (16) and (17) reduces to the Pflüger beam with the axial compressive force treated in Atanackovic (1997), that will be used in estimations of the influence of the small length scale parameter κ on the critical load.

Given $\kappa > 0$ and $a(t)$ being constant or not, the eigenvalue pair (λ_1, λ_2) of the system (15) and (14) or equivalently of the system (16) and (17) defines a set of curves $\phi_n,\ n = 1, 2, \ldots$ called interaction curves (see Antman, 1995). Our next goal is to find the lowest interaction curve (i.e. a curve corresponding to the lowest buckling mode) for the nano/micro beam with constant cross-section $a(t) = 1$, corresponding to the uniform beam of unit volume. In what follows we will assume that λ_1, λ_2 are positive. Next we present two possible ways to determine the interaction curves.

3.1. Standard procedure

In this subsection we derive an analytical form of a characteristic equation that determines the interaction curves of the uniform beam for $\kappa > 0$. Therefore we solve

$$\ddot{m} + \frac{\lambda_1 + \lambda_2(1-t)}{1 - \kappa^2[\lambda_1 + \lambda_2(1-t)]} m = 0 \tag{20}$$

subject to (17). Introducing the new independent variable

$$y = 2\frac{\kappa^2[\lambda_1 + \lambda_2(1-t)] - 1}{\kappa^3\lambda_2}. \tag{21}$$

Eq. (20) becomes

$$\frac{d^2m}{dy^2} - \frac{1}{4}\left(1 + \frac{2}{\lambda_2\kappa^3 y}\right)m = 0. \tag{22}$$

Next we suppose a solution of (22) in the form

$$m(y) = \frac{\kappa^3\lambda_2}{2} y e^{-\frac{y}{2} + \frac{\kappa^2[\lambda_1+\lambda_2]-1}{2}} f(y), \tag{23}$$

where $f(y)$ is the function to be determined. Substituting (23) into (22) leads to the following linear differential equation for $f(y)$

$$y\frac{d^2f}{dy^2} + (2-y)\frac{df}{dy} - \left(1 + \frac{2}{\lambda_2\kappa^3}\right)y = 0. \tag{24}$$

If we introduce the following notation

$$\alpha = 1 + \frac{1}{2\lambda_2\kappa^3}, \tag{25}$$

the general solution to (24) reads (see Abramowitz and Stegun, 1970; Lebedev, 1965)

$$f(y) = C_1\Phi(\alpha, 2, y) + C_2\Psi(\alpha, 2, y), \tag{26}$$

where C_1 are C_2 are arbitrary constants. Also, in (26) $\Phi(\alpha, 2, y)$ stands for the confluent hypergeometric function defined by

$$\Phi(\alpha, 2, y) = \sum_{k=0}^{\infty} \frac{(\alpha)_k}{(2)_k}\frac{y^k}{k!}, \tag{27}$$

while $\Psi(\alpha, 2, y)$ stands for the confluent hypergeometric function of the second kind given by (see Lebedev, 1965)

$$\Psi(\alpha, 2, y) = \frac{1}{\Gamma(\alpha-1)}\left\{\sum_{k=0}^{\infty}\frac{(\alpha)_k}{(1+k)!}\frac{y^k}{k!}[\psi(\alpha+k) - \psi(1+k) - \psi(2+k) + \ln y]\right\} + \frac{1}{y\Gamma(\alpha)}. \tag{28}$$

In (27) and (28) we used $\Gamma(\cdot)$ to denote the Euler gamma function, $(\alpha)_k$ is the Pochhammer symbol defined in the usual way

$$(\alpha)_k = \alpha(\alpha+1)\cdots(\alpha+k-1), \quad k > 0$$

with $(\cdot)_0 = 1$, and $\psi(\cdot)$ is the logaritmic derivative of the gamma function i.e. $\psi(\cdot) = \Gamma'(\cdot)/\Gamma(\cdot)$. Since $\alpha > 0$ the functions $\Phi(\alpha, 2, y)$ and $\Psi(\alpha, 2, y)$ are linearly independent. Taking into account (21), (23) and (26) the general solution of (20) reads

$$m(t) = e^{\frac{t}{\kappa}}\{\kappa^2[\lambda_1 + \lambda_2(1-t)] - 1\} \times \left\{C_1\Phi\left(\alpha, 2, 2\frac{\kappa^2[\lambda_1 + \lambda_2(1-t)] - 1}{\kappa^3\lambda_2}\right) + C_2\Psi\left(\alpha, 2, 2\frac{\kappa^2[\lambda_1 + \lambda_2(1-t)] - 1}{\kappa^3\lambda_2}\right)\right\}. \tag{29}$$

The solution (29) can also be obtained if this problem is treated as a special case of the one presented in Polyanin and Zaitsev (2003). By enforcing the boundary conditions (17) we find that the nontrivial solutions exist iff

$$\{\kappa^2[\lambda_1+\lambda_2]-1\}\{\kappa^2\lambda_1 - 1\}\left\{\Phi\left(\alpha, 2, 2\frac{\kappa^2[\lambda_1+\lambda_2]-1}{\kappa^3\lambda_2}\right)\Psi \times \left(\alpha, 2, 2\frac{\kappa^2\lambda_1 - 1}{\kappa^3\lambda_2}\right) - \Phi\left(\alpha, 2, 2\frac{\kappa^2\lambda_1 - 1}{\kappa^3\lambda_2}\right)\Psi \times \left(\alpha, 2, 2\frac{\kappa^2[\lambda_1+\lambda_2]-1}{\kappa^3\lambda_2}\right)\right\} = 0. \tag{30}$$

Eq. (30) presents the characteristic equation that determines the critical loads (λ_1, λ_2) of the beam having the unit cross-sectional area for given κ.

3.2. Numerical solution of eigenvalue problem

Following the observation given in the introduction we now give the original boundary value problem (16) and (17) a numerical treatment *ab initio*. Thus, in order to determine the critical loads we apply the numerical method directly to (16) and (17) as suggested in Goodman (1965). Namely, given $\kappa > 0$ and $\lambda_1 > 0$, we put $\lambda = \sqrt{\lambda_2}$, and start with an initial guess for λ say λ^0. Next we integrate (16), with the initial conditions $(17)_1$ and (19), together with backward integration of the equation adjoint to (16) with a variable say m^*, which has to be done with the following starting values

$$m^*(1) = 1, \quad \dot{m}^*(1) = 0. \tag{31}$$

The increment of λ reads

$$\Delta\lambda = \frac{m(1)}{\int_0^1 \frac{2\lambda(1-u)m(u)\dot{m}^*(u)du}{\left[1-\lambda_1\kappa^2-\lambda^2\kappa^2(1-u)\right]^2}}. \tag{32}$$

The procedure is repeated for $\lambda + \Delta\lambda$ until the convergence is achieved, (see Appendix A for details).

4. Optimization problem and its solution

The main goal of this section is to derive governing equations describing the optimal shape of the beam. In order to do that we suppose that κ and (λ_1, λ_2) are given. Then we say the beam has

the optimal shape if it is so shaped that any other beam of the same length and smaller volume will buckle under the same load (λ_1, λ_2). Also, we define a set of admissible cross-sectional area functions U as a set of continuously differentiable functions on the closed interval $[0,1]$ satisfying (18). With these definitions we can state an optimization problem in the following way: given $\kappa > 0$ and $(\lambda_1^*, \lambda_2^*)$ find $a^*(t) \in U$ such that the integral (12) is minimal and that the eigenvalue pair (λ_1, λ_2) belonging to the lowest interaction curve of (16) and (17) with $a(t) = a^*(t)$ equals $(\lambda_1^*, \lambda_2^*)$. In other words, we wish to find the distribution of material along the micro/nano beam so the beam is of minimal volume and stable against buckling i.e. $\min_a w$. We chose to use the Pontryagin maximum principle as a mathematical tool for deriving the governing equations. In order to apply the Pontryagin maximum principle we introduce the variables

$$x_1 \equiv m, \quad x_2 \equiv \dot{m},$$

so that Eqs. (16) and (17) become

$$\dot{x}_1 = x_2, \quad \dot{x}_2 = -\frac{\lambda_1 + \lambda_2(1-t)}{a^2 - \kappa^2[\lambda_1 + \lambda_2(1-t)]} x_1 \tag{33}$$

subject to

$$x_1(0) = 0, \quad x_1(1) = 0. \tag{34}$$

We note that the condition (34) leads to unimodal optimization. With respect to this we introduce the costate variables p_1, p_2 to form Hamiltonian $\mathcal{H}$, (the Pontryagin function)

$$\mathcal{H} = a + p_1 x_2 - p_2 \frac{\lambda_1 + \lambda_2(1-t)}{a^2 - \kappa^2[\lambda_1 + \lambda_2(1-t)]} x_1 \tag{35}$$

and find the optimal distribution of the material a as a solution of the equation $\partial\mathcal{H}/\partial a = 0$, leading to

$$1 + \frac{2a p_2 x_1 [\lambda_1 + \lambda_2(1-t)]}{\{a^2 - \kappa^2[\lambda_1 + \lambda_2(1-t)]\}^2} = 0. \tag{36}$$

The corresponding costate equations and the natural boundary conditions read

$$\dot{p}_1 = \frac{\lambda_1 + \lambda_2(1-t)}{a^2 - \kappa^2[\lambda_1 + \lambda_2(1-t)]} p_2, \quad \dot{p}_2 = -p_1 \tag{37}$$

and

$$p_2(0) = 0, \quad p_2(1) = 0. \tag{38}$$

Comparing (33) and (34) with (37) and (38) we conclude that there is the connection between the state and costate variables

$$p_1 = x_2, \quad p_2 = -x_1 \tag{39}$$

reducing the optimality condition (36) to

$$1 - \frac{2a[\lambda_1 + \lambda_2(1-t)]}{\{a^2 - \kappa^2[\lambda_1 + \lambda_2(1-t)]\}^2} x_1^2 = 0. \tag{40}$$

Eq. (36) can be cast in the form of a depressed quartic equation

$$a^4 - 2a^2\kappa^2[\lambda_1 + \lambda_2(1-t)] - 2a[\lambda_1 + \lambda_2(1-t)]x_1^2 + \kappa^4[\lambda_1 + \lambda_2(1-t)]^2 = 0, \tag{41}$$

which can be solved by the use of the Lodovico Ferrari method. Note, that from (35) and (39), by the use of (40) and (18) we calculate

$$\frac{\partial^2\mathcal{H}}{\partial a^2} = \frac{3a^2 + \kappa^2[\lambda_1 + \lambda_2(1-t)]}{a\{a^2 - \kappa^2[\lambda_1 + \lambda_2(1-t)]\}} > 0$$

and conclude that the necessary condition for minimum of $\mathcal{H}$ with respect to a is satisfied. This eliminates the other possible choices of type (39). Thus, the optimal shape of the beam $a(t) = a^*(t)$, follows as a solution of the boundary value problem given by (33), (34) and (41).

We make two remarks here. First we note that when $\kappa = 0$ and $\lambda_1 = 0$, we recover the optimality condition for the Pflüger beam posed in the sense of the classical Bernoulli–Euler elastica theory (see Atanackovic and Simic, 1999). Secondly, the influence of nonlocal theory as well as the generalization of the classical elastica theory shown in Spasic and Glavardanov (2009), lead to a complicated two point boundary value problem since the optimality conditions are given in complex form. Namely, in both cases the posed boundary value problems require the solution of a cubic or quadratic equation. However, it appears that the explicit form of these solutions are not suitable for further numerical analysis. As a consequence we use an alternative procedure that avoids to many "if then else" conditions required in each step of integration of the two point boundary value problem (33) and (34) with (41) solved explicitly by Ferrari's method. Namely, we differentiate the optimality condition (40) and then use $(33)_1$ and (40) in order to obtain an expression for $\dot{a}$ as a function of a and x_2. Next the optimality condition (40) is used to eliminate the state variable x_1 from $(33)_2$. In this way the original optimization problem given by (33) and (40) is transformed into the following one

$$\dot{a} = \frac{(\pm 1)\sqrt{2a[\lambda_1 + \lambda_2(1-t)]}x_2 - \frac{\lambda_2}{2}\left[\kappa^2 + \frac{a^2}{[\lambda_1 + \lambda_2(1-t)]}\right]}{\frac{3}{2}a + \frac{\kappa^2}{2a}[\lambda_1 + \lambda_2(1-t)]},$$

$$\dot{x}_2 = (\pm 1)\frac{[\lambda_1 + \lambda_2(1-t)]}{\sqrt{2a[\lambda_1 + \lambda_2(1-t)]}}$$

and further to

$$\dot{a} = \frac{\{2a[\lambda_1 + \lambda_2(1-t)]\}^{3/2}x_2 - \lambda_2 a\{\kappa^2[\lambda_1 + \lambda_2(1-t)] + a^2\}}{[\lambda_1 + \lambda_2(1-t)]\{\kappa^2[\lambda_1 + \lambda_2(1-t)] + 3a^2\}},$$

$$\dot{x}_2 = -\sqrt{\frac{[\lambda_1 + \lambda_2(1-t)]}{2a}}. \tag{42}$$

The corresponding boundary conditions now follow from (34) and (40)

$$a(0) = \kappa\sqrt{\lambda_1 + \lambda_2}, \quad a(1) = \kappa\sqrt{\lambda_1}. \tag{43}$$

Note that Eq. (42) corresponds to the case $m(t) = x_1(t) \neq 0$ for $t \in (0,1)$ leading to the lowest buckling mode. The boundary value problem (42) and (43) can easily be solved by shooting method yielding the optimal distribution of the material along the micro/nano beam $a^*(t)$.

5. Numerical results

In this section we present numerical results concerned with the critical load of the uniform micro/nano beam, the optimal shape of it as well as the postbuckling behavior of both uniform and optimal micro/nano beam for the same load and small length scale beam parameter κ.

5.1. Critical load

Here we present the critical load of the uniform Pflüger micro/nano beam that is obtained by a numerical solution of the corresponding linear eigenvalue problem for several values of system parameters. In particular, we chose several values for parameter κ and then for fixed λ_1 we find the lowest value of λ_2 that satisfies either (30) or was obtained by the iterative procedure given in Section 3.2 and Appendix A. In that way we determine the lowest interaction curves (the curves corresponding to the lowest buckling mode) presented in Fig. 2. As expected the results for the critical load obtained by numerical solutions of (30) and the numerical procedure given in Section 3.2 and Appendix A, coincide but the latter is more tractable. As the matter of fact for κ belonging to a

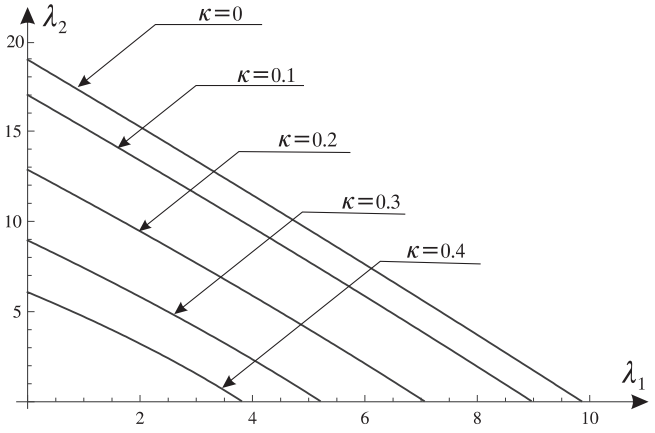

Fig. 2. Interaction curves for several values of the small length scale parameter.

small neighborhood of zero it was very difficult to solve (30), so the lowest interaction curve, corresponding to that region was obtained by the numerical method of Goodman.

We make a few comments on the interaction curves in Fig. 2. First, we analyze the case $\kappa = 0$ that corresponds to the classical Bernoulli–Euler beam. It is worth noting that in this case the interaction curve agrees very well with the corresponding critical values presented in Atanackovic (1997), see Table 13.12.1 on p. 185 therein, with differences that are less then 10^{-3}. Next, for the beam compressed only by a force ($\lambda_1 \neq 0,\ \lambda_2 = 0$) the critical load obtained as a solution to (30) for $\lambda_2 = 0$ agrees very well with the analytical solution $\lambda_1 = \pi^2/(1+\kappa^2\pi^2)$ that follows from (20) and (17) and is in agreement with the previously reported results (see Sudak, 2003; Wang et al., 2006). Finally we comment on the Pflüger micro/nano beam described by the Eringen's model for constitutive bending curvature relationship ($\kappa \neq 0$). In Fig. 2 we show four interaction curves obtained for $\kappa \in \{0.1, 0.2, 0.3, 0.4\}$. From the interaction curves presented we conclude that by increasing the small length scale parameter κ the critical load decreases. It is also worth noting an interesting property. Namely, fixing λ_1 (or λ_2) and increasing κ the influence of the change of κ on the change of the critical value λ_2 (or λ_1) is described by a nonmonotonic function. This property deserves more investigation.

5.2. Optimal shape

The main goal of this subsection is to analyze the influence of the micro/nano beam parameter κ on the optimal shape and savings in material along the interaction curve with respect to the uniform beam. In order to determine the optimal shape of the beam the boundary problem given by (42) and (43) was solved numerically. Once the optimal shape was determined, the volume of the optimal beam follows from (12). Note that the buckling mode can also be determined if the system (42) and (43) is solved along the Eqs. $(15)_{5,6}$ $(14)_{2,4}$ and (40).

We mention an important fact. Namely, for $\kappa = 0$ (the classical Bernoulli–Euler beam theory) the boundary conditions (43) imply that the cross-sectional area of the optimal beam will vanish at both ends of the beam. Physically this is an unwanted property. For micro/nano beam, i.e., for $\kappa > 0$ the cross-sectional areas at the ends of the optimal beam are greater then zero! This means that the nonlocal constitutive bending curvature relationship regularizes the optimal solution. We mention that the same effect is observed in Atanackovic et al. (in press). The boundary conditions (43) also show that $a(0) > a(1)$ for given λ_1, λ_2 and κ greater then zero and that the increase in κ leads to the increase in the cross sectional areas at both ends of the optimal beam.

Next we analyze several specific examples, numerically.

Since the main goal of optimization is to reduce the volume, remaining at the same time the critical loads unchanged, we will perform all the analysis along the interaction curves corresponding to the uniform beam (see Fig. 2). In order to comment on the optimal shape of the beam we chose $\kappa = 0.1$ and two points on the interaction curve say $(\lambda_1 = 1,\ \lambda_2 = 15.194)$, $(\lambda_1 = 8,\ \lambda_2 = 1.953)$. The corresponding optimal shapes for these two points are given in Fig. 3(a) and (b), respectively. Both shapes satisfy (18). From Fig. 3. we can conclude that there exists only one local extremum. We also note that since the point $(\lambda_1 = 1,\ \lambda_2 = 15.194)$ is relatively close to $(\lambda_1 = 0,\ \lambda_2 = 18.957)$, Fig. 3(a) qualitatively presents the shape of the optimal beams loaded dominantly by the uniformly distributed follower type of load. In a similar way it follows that Fig. 3(b) presents the shape of the optimal beam loaded dominantly by a concentrated force.

Next, we analyze the maximal value of the cross-sectional area $a_{\max}$ and its location t^* on the beam axis.

From Fig. 4. it follows that for $\kappa \in \{0.01, 0.1, 0.2, 0.3\}$ the increase in λ_1 along the interaction curves, $0 < \lambda_1 < \pi^2/(1+\kappa^2\pi^2)$, causes the decrease in the maximal value of the cross-sectional area $a_{\max}$. However, for $\kappa = 0.4$ the increase in λ_1 first causes $a_{\max}$ to increase and than to decrease. Note that the changes of $a_{\max}$ along all the interaction curves are relatively small and that these changes decrease when κ increases (see Fig. 4).

Fig. 5 shows that for $\kappa \in \{0.01, 0.1, 0.2, 0.3, 0.4\}$, the coordinate t^*, that measures how far the maximal cross-sectional area is from the left end of the beam, increases if λ_1 increases along the interaction curves. We note that the higher slopes of $t^*(\lambda_1)$ along the interaction curves correspond to the higher values of κ. Also t^* never

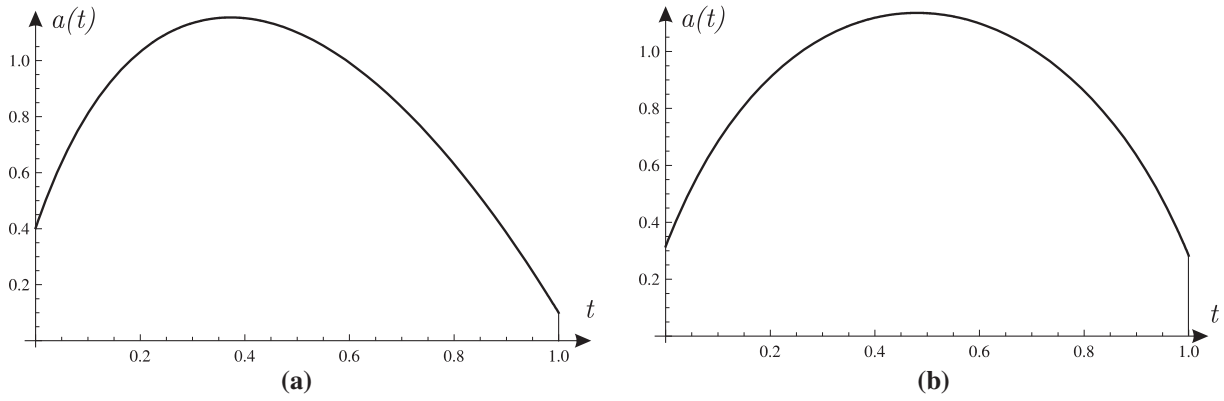

Fig. 3. The optimal shapes of the beam for $\kappa = 0.1$, $\lambda_1 = 1$, $\lambda_2 = 15.194$, (a) and $\kappa = 0.1$, $\lambda_1 = 8$, $\lambda_2 = 1.953$ (b).

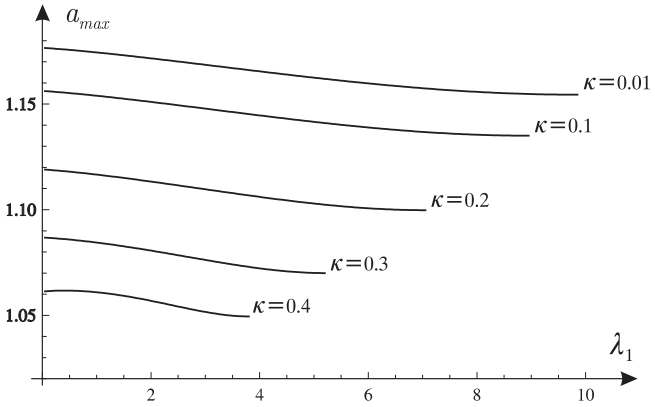

Fig. 4. The maximal cross-sectional areas along interaction curves.

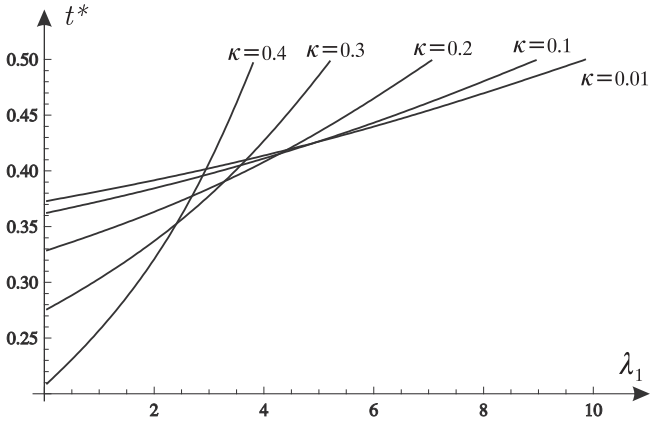

Fig. 5. The locations of maximal cross-sectional area of the optimal beam along interaction curves.

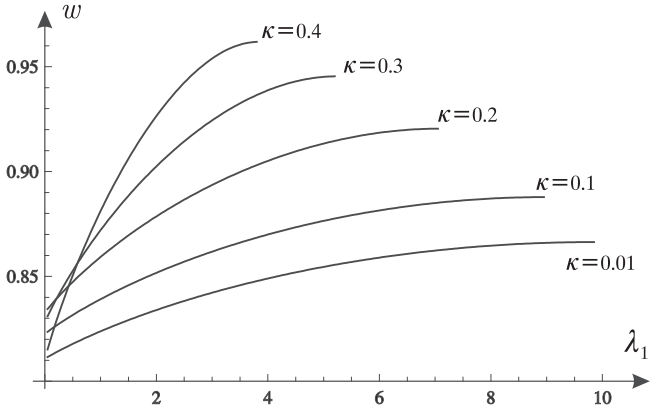

Fig. 6. The volume of the optimal beam along interaction curves.

exceeds 0.5 meaning that the maximal cross section of the optimal Pflüger micro/nano beam remains on the left part of the beam. We also conclude that the changes of t^* along all the interaction curves are significant and that these changes increase when κ increases.

Finally we present the savings in material obtained if the optimal beam is used instead of the uniform one. The volumes of optimal beams are denoted by w and will be given for several values of κ and, as before, with respect to the interaction curves shown in Fig. 2. The numerical results are presented in Fig. 6.

Table 1
Range of savings in material along the interaction curves.

κ	Range of savings (%)
0.01	13.37–18.93
0.1	11.22–17.75
0.2	7.96–16.73
0.3	5.47–17.19
0.4	3.82–18.98

From Fig. 6 we conclude that for any fixed $\kappa \in \{0.01, 0.1, 0.2, 0.3, 0.4\}$ the volumes of the optimal beams along the interaction curves increase. The savings in material are determined by $1-w$. Table 1. shows the range of savings in material along the interaction curves depending on κ. From Fig. 6 and Table 1. one can conclude that the optimal beams loaded dominantly by the uniformly distributed follower type of load are more efficient than the optimal beams loaded dominantly by a concentrated force. It is worth noting that the increase of κ increases this effect.

Finally, let us fix the value of λ_1 and allow the parameters κ and λ_2 to vary. Then from Fig. 6 it follows that the increase in κ leads to the decrease in savings if λ_1 does not belong to a neighborhood of zero.

5.3. Postbuckling behavior

In this subsection we analyze the postbuckling behavior of the uniform and the optimal beam for the same load and beam parameter κ. In order to do so let $(\lambda_1^*, \lambda_2^*)$ be a point on the interaction curve corresponding to given κ (see Fig. 2) and $a^*(t)$ be the cross-sectional area of optimal beam corresponding to $(\lambda_1, \lambda_2) = (\lambda_1^*, \lambda_2^*)$. If we chose λ_1 to be a bifurcation parameter and introduce the load increment $\Delta\lambda_1$ just to pass the stability boundary, the postbuckling behavior of both uniform and optimal beam is determined as a nontrivial solution of the nonlinear problem (13) and (14) with $(\lambda_1, \lambda_2) = (\lambda_1^* + \Delta\lambda_1, \lambda_2)$ for $a(t) = 1$ and $a(t) = a^*(t)$, respectively.

In order to perform numerical calculations we set $\kappa = 0.1$, $\Delta\lambda_1 = 0.05$ and select two points $(\lambda_1^* = 1,\ \lambda_2^* = 15.194)$, $(\lambda_1^* = 8,\ \lambda_2^* = 1.953)$ on the interaction curve. The corresponding postbuckling shapes are given in Fig. 7.

From the curves presented in Fig. 7 we conclude that for the same load and small length scale beam parameter, the maximal displacement in the lateral direction of the uniform beam is greater then the one corresponding to the optimal beam, while the latter is of smaller volume. Namely, the volume of the optimal beam for $\kappa = 0.1,\ \lambda_1^* = 1,\ \lambda_2^* = 15.194$, shown in Fig. 3a, reads $w_{\min} = w^* = 0.838$. If one introduces the uniform beam of the same volume as the optimal one and put $a(t) = \mathbf{a}_{sv} = 0.838$ in the linearized problem (16) and (17) for $\kappa = 0.1$ and $\lambda_1^* = 1$ one obtains the critical load $\lambda_2^* = 10.125$. Then one can conclude that while the optimal beam of the volume $w_{\min}$ buckles at $(\lambda_1, \lambda_2) = (1, 15.194)$, for the same load the uniform beam of the same volume as the optimal one will be very far in the postcritical region.

Referring to Fig. 7 again, one can observe that the maximal lateral displacement of the optimal beam is obtained on the right part of the beam. This is quite expectable if we recall the shape of the optimal beam (see Fig. 3).

At the end we comment on the fact that the postbuckling shapes are obtained for $\Delta\lambda_1 > 0$. This suggests that the supercritical bifurcation occurs for both optimal and uniform beam. Moreover, calculations show that along the whole interaction curve for $\kappa = 0.1$ only supercritical bifurcation occurs. We note that the similar results could be obtained if we chose λ_2 as a bifurcation parameter.

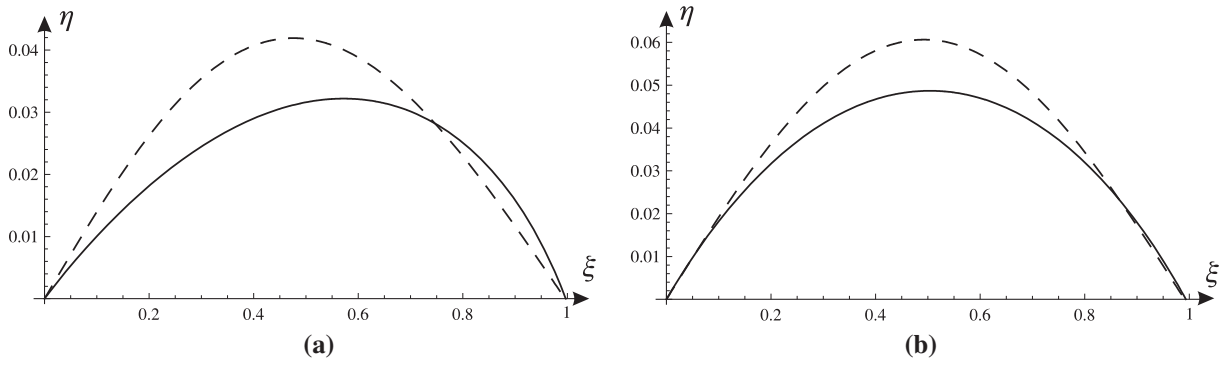

Fig. 7. The postbuckling shapes of the uniform (dashed line) and optimal beam for $\kappa = 0.1,\ \lambda_1 = 1,\ \lambda_2 = 15.194$, (a) and $\kappa = 0.1,\ \lambda_1 = 8,\ \lambda_2 = 1.953$ (b).

6. Conclusion

In this paper we treated a micro/nano beam pinned at both ends and loaded by a concentrated compressive force and the uniformly distributed follower type of load. For the constitutive equation, that take into account nano effects, Eringen's model for bending curvature relationship is used. The main results of this paper are:

1. The system of six nonlinear first order ordinary differential equations (13) and (14) describing the deformations of the micro/nano beam with a variable cross-section is derived.
2. By linearizing the system (13) and (14) we obtained the system (16) and (17) that determines the stability boundary of the micro/nano beam with a variable cross-section. As a special case we derived the characteristic equation (30) that determines the stability boundary of the uniform beam in closed form. We believe that this result is new. Along with that we used a known and suitable numerical method for obtaining the stability boundary directly from the system (17) and (20).
3. By using the characteristic equation (30) and numerical method presented in Appendix A we determined the interaction curves for several values of a small length scale parameter. The results are presented in Fig. 2 showing that the increase in the small length scale parameter decreases the critical load.
4. We used the Pontryagin maximum principle to derive necessary conditions for optimality and the corresponding governing equations (42) and (43) that are suitable for numerical treatment and make the problem of finding the optimal shape of the nano beam more tractable.
5. By solving the governing equations (42) and (43) numerically we determined the characteristic optimal shapes of the Pflüger micro/nanobeam for two different sets of load and beam parameters (see Fig. 3). We also determined the volume of the optimal beam along the interaction curves corresponding to different values of the small scale length parameter κ. The results presented in Fig. 6 show that the savings in material along the interaction curves decrease as λ_1 increases. This means that the optimal beams loaded dominantly by a uniformly distributed follower type of load are more efficient than the optimal beams loaded dominantly by a concentrated force. We note that the increase of κ increases this effect.
6. We determined the postcritical shape of the optimal and uniform beam. The results show that the larger deflection occurs in the case of the uniform beam (see Fig. 7). Also, the numerical results for $\kappa = 0.1$ suggest that supercritical bifurcation occurs along the interaction curve for both uniform and optimal beam.
7. Our results show that for $\kappa \in \{0.01, 0.1, 0.2, 0.3, 0.4\}$ the savings in material obtained by using the optimal shape of the beam are varying from 3.82% to 18.98% (see Table 1).

Acknowledgement

This research was supported by Serbian Ministry of Science Grants 174016 and 174005.

Appendix A. Numerical solution of eigenvalue problem (16) and (17).

We start with (16), by rewriting it in the form (33) with $a = 1$ and introduced $\lambda^2 = \lambda_2$. We assume the initial data $(34)_1$ and from (19), $x_2(0) = 1$. It is also assumed $\lambda = \lambda^*$. Now, Eq. (33) can be integrated as an initial value problem, and the solution denoted by $x_i^*(t),\ (i = 1, 2)$. In general it will be found that the computed value $x_1^*(1)$ differs from zero, representing the condition $(34)_2$. To obtain the correct solution the value of $x_1^*(1)$ must be made as small as possible. By defining $\delta x_i(t) = x_i(t) - x_i^*(t)$ and $\delta\lambda = \lambda - \lambda^*$ and than substituting it into (33) there results to a first approximation

$$\delta\dot{x}_1 = \delta x_2, \quad \delta\dot{x}_2 = -\frac{\lambda_1 + \lambda^{*2}(1-t)}{1-\kappa^2\left[\lambda_1 + \lambda^{*2}(1-t)\right]}\delta x_1 - \frac{2\lambda^*(1-t)x_1}{\left\{1-\kappa^2\left[\lambda_1 + \lambda^{*2}(1-t)\right]\right\}^2}\delta\lambda.$$

These are the equations of differential corrections. The equations adjoint to them read

$$-\dot{z}_1 = -\frac{\lambda_1 + \lambda^{*2}(1-t)}{1-\kappa^2\left[\lambda_1 + \lambda^{*2}(1-t)\right]}z_2, \quad -\dot{z}_2 = z_1,$$

which are to be solved only once by backward integration subject to the initial conditions $z_1(1) = 1,\ z_2(1) = 0$. According to Goodman (1965) the relation between δx_i's and z_i's reads

$$-x_1^*(1) = -\delta\lambda\int_0^1 \frac{2\lambda^*(1-t)x_1^* z_2 dt}{\left\{1-\kappa^2\left[\lambda_1 + \lambda^{*2}(1-t)\right]\right\}^2}.$$

Substituting the numerical solutions of the initial value problems into this equation and solving it for $\delta\lambda$ the improved values of λ are obtained. The suggested procedure for the Pflüger micro/nano beam was implemented on PC. The integral in (32), was calculated numerically while two initial value problems were solved by the use of standard Runge Kutta integrator with fixed step size. Note that only a few steps are necessary. For the illustration we show the sequence for $\lambda = \sqrt{\lambda_2}$, for the values $\kappa = 0.05,\ \lambda_1 = 9$ starting from $\lambda^0 = 1$. It reads $\lambda^1 = 1.129,\ \lambda^2 = 1.122,\ \lambda^3 = 1.122$. More on this quite efficient successive iterations method that is truly equivalent to Newton's method can be found in the cited paper of Goodman (1965).

References

Abramowitz, M., Stegun, I.A., 1970. Handbook of Mathematical Functions. Dover.

Antman, S.S., 1995. Nonlinear Problems of Elasticity. Springer, New York.

Atanackovic, T.M., 1997. Stability Theory of Elastic Rods. World Scientific, Singapore.

Atanackovic, T.M., Simic, S.S., 1999. On the optimal shape of a Pflü ger column. Eur. J. Mech. A/Solids 18, 903–913.

Atanackovic, T.M., Novakovic, B., Vrcelj, Z. in press. Shape optimization against buckling of micro and nano rods. Arch. Appl. Mech.

Atanackovic, T.M., Novakovic, B., Vrcelj, Z., 2012. Application of Pontryagin's principle to bimodal optimization of nano rods. IJSSD 12, 1250012 (11p).

Challamel, N., Wang, C.M., 2010. On lateral-torsional buckling of non-local beams. Adv. Appl. Math. Mech. 2, 389–398.

Chow, S.N., Hale, J.H., 1982. Methods of Bifurcation Theory. Springer, Berlin.

Eringen, A.C., 1983. On differential equations of nonlocal elasticity and solutions of screw dislocation and surface waves. J. Appl. Phys. 54, 4703–4710.

Goodman, T.R., 1965. The numerical solutions of eigenvalue problems. Math. Comput. 19, 462–466.

Kovari, K., 1969. Raumlishe Verzweingungsprobleme des dunnen elastischen Stabes mit endlichen Verformungen. Ingineur Archiv 37, 393–416.

Ke, L.-L., Wang, Y.-S., 2011. Flow-induced vibration and instability of embedded double-walled carbon nanotubes based on a modified couple stress theory. Physica E 43, 1031–1039.

Lebedev, N.N., 1965. Special Functions and their Applications. Prentice-Hall, Englewood Cliffs, NJ.

Lee, H.-L., Chang, W.-J., 2008. Free transverse vibration of the fluid-conveying single-walled carbon nanotube using nonlocal elastic theory. J. Appl. Phys. 103, 024302(4pp).

Lu, P., Lee, H.P., Lu, C., Zhang, P.Q., 2007. Application of nonlocal beam models for carbon nanotubes. Int. J. Solids Struct. 44, 5289–5300.

Ma, H.M., Gao, X.-L., Reddy, J.N., 2008. A microstructure-dependent Timoshenko beam model based on a modified couple stress theory. J. Mech. Phys. Solids 56, 3379–3391.

Peddieson, J., Buchanan, G.R., McNitt, R.P., 2003. Application of non-local continuum models to nanotechnology. Int. J. Eng. Sci. 41, 305–312.

Plaut, R.H., 2004. Postbuckling and vibration of end-supported elastica pipes conveying fluid and columns under follower loads. J. Sound Vib. 289, 264–277.

Polyanin, A.D., Zaitsev, A.F., 2003. Handbook of Exact Solutions for Ordinary Differential Equations. Chapman & Hall/CRC, Boca Raton.

Spasic, D.T., Glavardanov, V.B., 2009. Does generalized elastica lead to bimodal optimal solutions? Int. J. Solids Struct. 46, 2939–2949.

Sudak, L.J., 2003. Column buckling of multiwalled carbon nanotubes using nonlocal continuum mechanics. J. Appl. Phys. 94, 7281–7287.

Tounsi, A., Heireche, H., Benzair, A., Mechab, I., 2009. Comment on 'vibration analysis of fluid-conveying double-walled carbon nanotubes based on nonlocal elastic theory'. J. Phys. Condens. Matter 21, 448001(3pp).

Wang, C.M., Zhang, Y.Y., Ramesh, S.S., Kitipornchai, S., 2006. Buckling analysis of micro- and nano-rods/tubes based on nonlocal Timoshenko beam theory. J. Phys. D: Appl. Phys. 39, 3904–3909.

Wang, Q., Wang, C.M., 2007. The constitutive relation and small scale parameter of nonlocal continuum mechanics for modelling carbon nanotubes. Nanotechnology 18, 075702(4pp).

Wang, L., 2009. Dynamical behaviors of double-walled carbon nanotubes conveying fluid accounting for the role of small length scale. Comput. Mater. Sci. 45, 584–588.

Whittaker, E.T., Watson, G.N., 1966. A course of Modern Analysis. Cambridge University Press.

Xiang, Y., Wang, C.M., Kitipornchai, S., Wang, Q., 2010. Dynamic instability of nanorods/nanotubes subjected to an end follower force. J. Eng. Mech. 136, 1054–1058.